Effects of Subcooling on Lengths of Propagating Normal Zones in the LHD Helical Coils

Effects of Subcooling on Lengths of Propagating Normal Zones in the LHD Helical Coils

Shinsaku Imagawa, *IEEE Member*, Hiroki Noguchi, Tetsuhiro Obana, Shinji Hamaguchi, Nagato Yanagi, and Toshiyuki Mito

Abstract—Propagation of a short normal zone was observed in a helical coil of the Large Helical Device when the coil was cooled with subcooled helium, the inlet and outlet temperatures of which are 3.2 K and below 4.0 K, respectively. The normal zone was induced at the bottom position of the coil. It propagated to only the downstream side of the current with recovery from the opposite side, and stopped after passing the outer equator of the torus. The induced balance voltage is obviously lower and the propagating time is shorter than those of propagating normal zones observed in the helical coil cooled with saturated helium at 4.4 K. According to the simulation of the propagation of a normal zone, it is considered that such a short normal zone at the current close to the minimum propagating current propagates without full transition to film boiling.

Index Terms—balance voltage, current diffusion, normal-zone propagation, oxidization, simulation.

I. INTRODUCTION

ONE pair of helical coils of the Large Helical Device (LHD) is the world's largest pool-cooled superconducting magnet, which has been operated for the research of fusion plasma since 1998 [1], [2]. The conductor of the coils consists of NbTi/Cu strands, a pure aluminum stabilizer, and a copper sheath, as shown in Fig. 1. The conductor surface is oxidized for enhancement of critical heat flux in nucleate boiling [3]. Because of the additional heat generation by slow current diffusion into the thick pure aluminum stabilizer, several one-side propagations of a normal zone were observed at around 11 kA, as shown in Fig. 2. The one side propagation is considered to be caused by electromagnetic interaction of the external magnetic field with the transfer current between the superconducting strands and the stabilizer [4]-[7]. In order to improve the cryogenic stability by lowering temperatures, an additional cooler was installed at the inlet of the coil in 2006 [8]. The inlet and outlet temperatures of the coils are lowered to 3.2 K and 3.8 K, respectively. We have observed the propagation of a short normal zone in the helical coils cooled with subcooled helium. Such short propagating normal zones were also observed in a model coil of the helical coil in the case it was cooled with subcooled helium [9]. The lengths of propagating normal zones in subcooled helium are shorter than in saturated helium in spite of the higher operating currents. The shorter length of the normal zone is caused by the quicker starting of recovery. This paper intends to summarize the features of propagating normal zones in subcooled helium and to clarify the reason for the quick recovery.
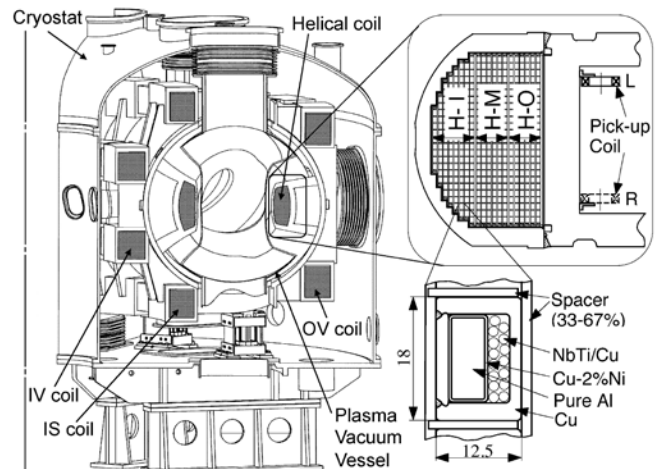

Fig. 1. Cross-section of the LHD cryostat and the helical coils, which consist of H-I, H-M, and H-O blocks. The turn number of each block is 150. [5]
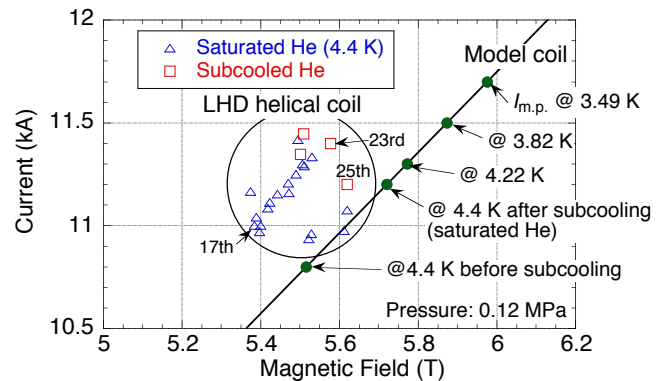

Fig. 2. Normal zone propagation currents of the LHD helical coil and minimum propagating current, $I_{m.p.}$, of the model coil. The magnetic fields of LHD are at the bottom position where most of the normal zones were initiated. In the model coil, the $I_{m.p.}$ in saturated helium is improved after being subcooled once, and the good condition is kept even after the coil quench.

II. EXPERIMENTAL RESULTS

A. Propagation of a Normal Zone in the LHD Helical Coil

Each helical coil, H1 or H2 is divided into three blocks, named H-I, H-M, and H-O from the inside, as shown in Fig. 1.

Each pair of the blocks in H1 and H2 coils is connected in series to each power supply. The balance voltage is the terminal voltage of H1 coil minus that of H2 coil for each block. During propagation of a normal zone, balance voltages are induced in all the blocks because of a current redistribution in the conductor from the superconducting strands to mainly the aluminum stabilizer at the normal zone. When a normal zone propagates in the H-I block, the voltage drop due to the resistance of the normal zone, V_R is expressed by [10]

$$V_R = e_I - \frac{\dot{M}_{Ik}}{\dot{M}_{Mk}} e_M = e_I - \frac{B_I I_M}{B_M I_I} e_M \equiv e_I - \frac{e_M}{\alpha} \qquad (1)$$

where e_j and I_j are the balance voltage and the current of j (=H-I or H-M) block. B_j is the magnetic field density induced by j block at the conductor where the normal zone propagates. α is given by $(B_M I_I)/(B_I I_M)$. α of 0.7 means that the normal zone propagates in the first layer in H-I [11], where the field is the highest. Figure 3a shows the balance voltages at the 25th propagation, and Fig. 3b shows V_R for α of 0.7, 0.8, and 0.9. Comparing the incline of the voltage at the startup and recovery with the other propagations [10], as shown in Fig. 4, α of 0.7 is the most suitable to get the reasonable V_R. The propagating time of the 17th propagation is the shortest among the propagations in saturated helium. According to the measurement with pickup coils along the helical coil, the normal zone was initiated at the bottom position of the helical coil. It propagated to the outer equator of the torus and stopped after passing the top position. The 23rd and 25th propagations occurred in subcooled helium. They were also initiated at the bottom, and stopped after passing the outer equator. As shown in Fig. 4, their propagation time and the reached length of normal zones are shorter than those of the 17th propagation in spite of the higher operating current.
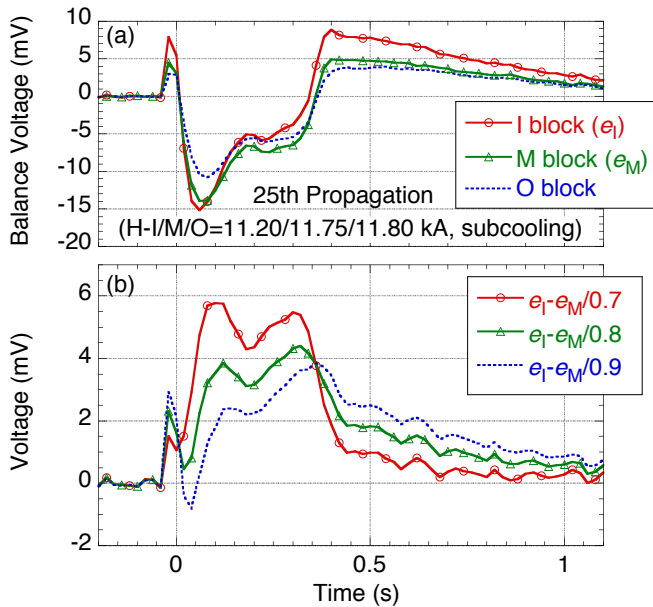

Fig. 3. Balance voltages (a) and their difference between H-I and H-M (b) at the 25th propagation of a normal zone in the LHD helical coil.
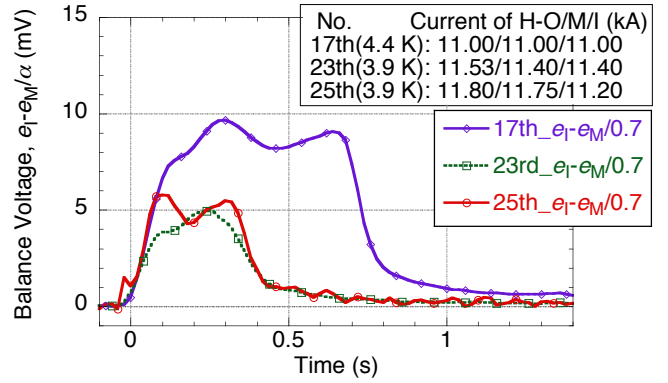

Fig. 4. The resistive voltage at 17th, 23rd, and 25th propagations of normal zones in the LHD helical coil.

B. Duration of Transition to Normal State

The voltage drop during propagation of a normal zone was measured in the model coil using voltage taps [9]. It can be fitted by exponential functions using the duration of transition to normal state, t_r, as shown in Fig. 5, also in the cases where the recovery starts before the current deeply diffuses into the aluminum stabilizer. At the front of a normal zone, high resistance is induced by slow current diffusion into the stabilizer [11], [12]-[15]. Such resistance decreases to a constant value with a time constant of 0.06 s, which is half of the characteristic time of the current diffusion into the stabilizer [11]. On the other hand, the primary time constant in recovery, in which the current diffuses from the stabilizer to the superconducting strands, is four times longer than that in propagation according to the theory [11]. In order to fit the experiments, another longer time constant in the order of 1.5 s must be considered. Such long time constant should be caused by coupling losses in the strands.

The resistive voltages calculated by the fitting equation with t_r=0.08 s at the propagation velocity of 6 m/s for the 17th propagation and t_r=0.02, 0.03, and 0.04 s at 7 m/s for the 25th propagation are shown in Fig. 6. The propagation velocities are assumed based on the data measured with pickup-coils for the cases where normal zones propagated over one pitch [10]. The shorter length of the normal zone in subcooled helium is caused by the quicker starting of recovery. Figure 6 shows that the recovery should start within 0.02-0.03 s after the normal transition in the 25th propagation. It is fairly shorter than the time constant of current diffusion into the aluminum stabilizer.

Figure 7 shows t_r in the model coil for different helium temperatures. Since t_r is slightly varied at the position of voltage taps, and t_r has a tendency to be elongated at the far positions from the heated point, the averaged values for six voltage taps in 0.32 to 1.13 m from the heater are shown. The minimum current for each temperature corresponds to the minimum propagating current. The t_r at a fixed temperature is longer at high currents, and the t_r at the minimum propagating current is shortened as the temperature is lowered. Short propagating normal zones with t_r =0.02-0.03 s were observed, too, in the model coil cooled with subcooled helium. Such a short normal zone can not propagate in saturated helium.
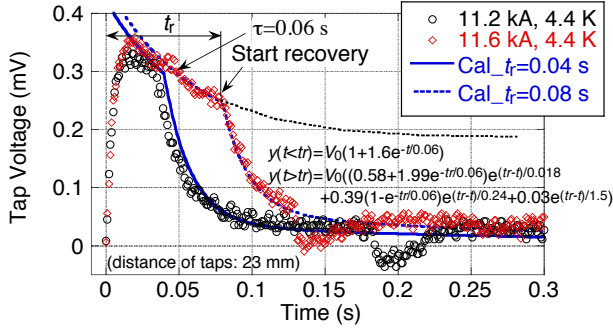
Fig. 5. Output of a pair of voltage taps, which is located at 0.49 m from the heated point, of the model coil for the current of 11.2 kA and 11.6 kA at saturated helium after being subcooled to 3.5 K.
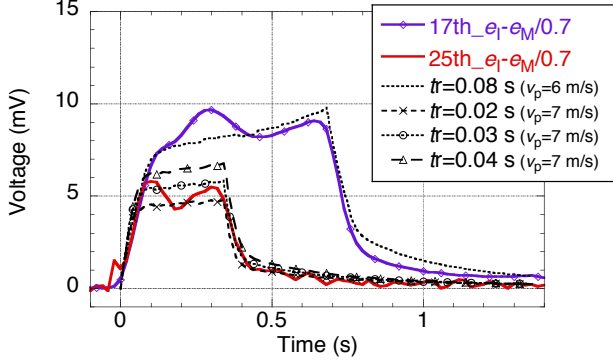

Fig. 6. Calculated resistive voltage at the 17th and 25th propagations. The stopping time of the propagation is set at 0.68 s and 0.34 s, respectively.
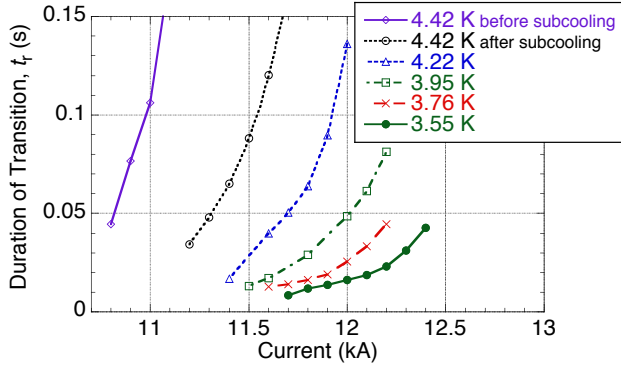

Fig. 7. Durations of transition to normal state in the model coil. They are averaged values of six voltage taps located at 0.32, 0.49, 0.65, 0.81, 0.97, and 1.13 m from the heated point. The cryogenic stability in saturated helium is clearly improved after being subcooled.

III. NUMERICAL ANALYSIS OF PROPAGATION

A. Analysis Model

In order to simulate propagating normal zones, a calculation model is proposed [7]. Since thermal conductivity in copper and aluminum is sufficiently high, the conductor is divided into 5 elements, as shown in Fig. 8, which are half of the copper sheath on the strands side (Cu1), NbTi/Cu strands and PbSn solder (SC), the CuNi layer between the strands and the aluminum stabilizer (CuNi), the aluminum stabilizer and the rest of the CuNi layer (Al), and half of the copper sheath on the stabilizer side (Cu2). The size and conditions of the analysis model is shown in Fig. 9. The pitch length of spacers between turns is 54 mm with the wetted surface of 67%, meaning that the cooled area is 36 mm, as shown in Fig. 9.

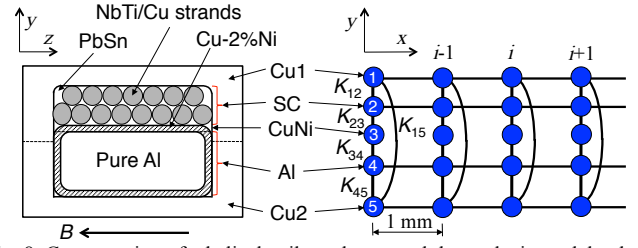The heat balance of the elements is solved with a finite differential method with the time step of 0.2 µs.

Fig. 8. Cross-section of a helical coil conductor and the analysis model, where K_{12}, K_{23}, K_{34}, K_{45}, and K_{15} are thermal conductances between the elements. Since the thermal conductivity of CuNi is low enough, the thermal conduction of CuNi in the longitudinal direction (x-direction) is ignored.
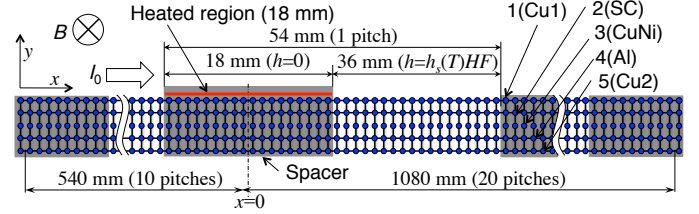

Fig. 9. The size and conditions of the analysis model. The external heat is input into Cu1 in the uncooled region around x=0. h is heat transfer in the calculation. $h_s(T)$ is given by Fig. 10, and HF is the efficiency of heat transfer.

B. Analysis Conditions

Since the transfer current between the strands and the stabilizer crosses the external magnetic field, a Hall electric field is induced in the longitudinal direction (x-direction). In these analyses, direct interaction between the Hall electric field and the transport current is assumed. The works by Hall effect is given by

$$W^{Al} = \int_0^\ell E_x I_x^{Al}(x)\,dx = \left(R_H^{Al} + R_H^{Cu}\right) B_z I_0^2 / 2a = W^{SC} \quad (2)$$

where E_x is Hall electric field by the transfer current, I_x^{Al} is the transport current in the aluminum stabilizer, R_H^{Al} is Hall coefficient of aluminum (1.022×10^{-10} m^3/C), R_H^{Cu} is Hall coefficient of copper (-0.54×10^{-10} m^3/C), j is current density, B_z is magnetic field, I_0 is transport current, l is length of transfer region, and a is width of the strands. The works by the Hall effect are negative at the upstream side of the transport current and positive at the downstream side. In addition, joule loss by the transfer current is given by $I_0^2(R(t)\,r)^{0.5}$ where $R(t)$ is resistance per unit length of the aluminum stabilizer, and r is contact resistance per unit length through the CuNi layer. The characteristic length of current transfer, l is given by $(r/R(t))^{0.5}$. In this analysis, l is set at 25 mm considering the high transient resistance of the aluminum during current diffusion. The normal zone is defined as the area in which the temperatures are higher than the current sharing temperature, T_{CS}. The middle of the current transfer region is set at the edge of the normal zone.

The transient heat generation during one-dimensional current diffusion into a stabilizer can be solved analytically [11], [12]. At first, the effective resistance of each element is estimated using the exponential decay time constant that is

calculated analytically. Next, the current of each element is calculated as four parallel electronic circuits. The fraction of current in the aluminum stabilizer is approximately 80%.

Thermal conductivity of copper in magnetic field at low temperatures is given with Wiedemann-Franz coefficient (2.443×10^{-8} WΩ/K^2) and the residual resistivity ratio (copper sheath: 180, copper in the strands: 63) [16]. Table 1 shows the thermal conductances between the elements. The "Ideal" values are derived from the conductances of the bulk materials by assuming that an average thickness of the solder around the strands is 0.2 mm. Since their actual values should be reduced because of contact resistance, the suitable values were surveyed to fit the calculated propagation velocities to the experiments with the model coil, in which B_z and T_{cs} at the testing area are 6.13 T and 5.70 K, respectively, at 12.0 kA. Heat transfer in liquid helium is fitted as shown in Fig. 10 from the experimental data with a conductor sample at vertical position. The power law for the nucleate boiling is set at 1.5 [17]. Specific heat of NbTi is referred from literature [18].
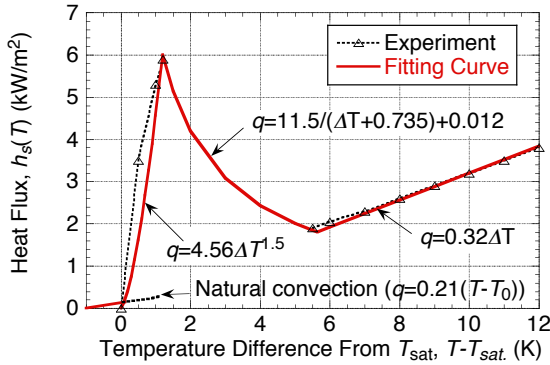
Fig. 10. Heat flux from a conductor sample of the helical coil in saturated liquid helium at 4.2 K. The conductor surface is oxidized.

TABLE I MAJOR PARAMETERS FOR SIMULATION OF A NORMAL ZONE.

Parameters		Ideal	Suitable values for cal.
K_{12}	(W/m/K)	194.5	100
K_{23}	(W/m/K)	109.9	20
K_{34}	(W/m/K)	233.5	100
K_{45}	(W/m/K)	108.3	50
HF for 4.4 K before subcooling		–	0.75
HF for 4.4 K after subcooling		–	0.95

HF: efficiency of heat transfer.

C. Calculated Results

The suitable parameters for K_{12} to K_{45} and heat transfer efficiency, HF were surveyed to simulate both the minimum propagating currents with an error less than 0.1 kA and the propagation velocities with an error less than 10%. In the "Ideal" case, HF can not be determined because of strong current dependence. A suitable set of K_{12} to K_{45} depends on HF. The most suitable set is shown in Table 1. The dependence of propagation velocity on the current is better fitted with fairly small K_{23}, which suggests insufficient contact between the strands and the CuNi layer. Although short propagating normal zones with t_r~0.02 s can not be simulated yet, a representative result for quick recovery with t_r~0.04 s is shown in Fig. 11. The highest temperature of Cu1 except for the heated region is lower than 7.3 K that is in the transition

region from nucleate boiling to film boiling. In the case the reached temperature in the normal zone is higher, the recovery starts more slowly. The main cause for the quick recovery is low reached temperature in the normal zone. Since the reached temperature of Cu1 at t_r~0.02 s must be lower than that at t_r~0.04 s, such a short normal zone is considered to propagate without full transition to film boiling. In other words, a normal zone can propagate under the good heat transfer due to the temperature rise in the oxidized surface. Transient heat transfer must be taken into account for the further discussion.
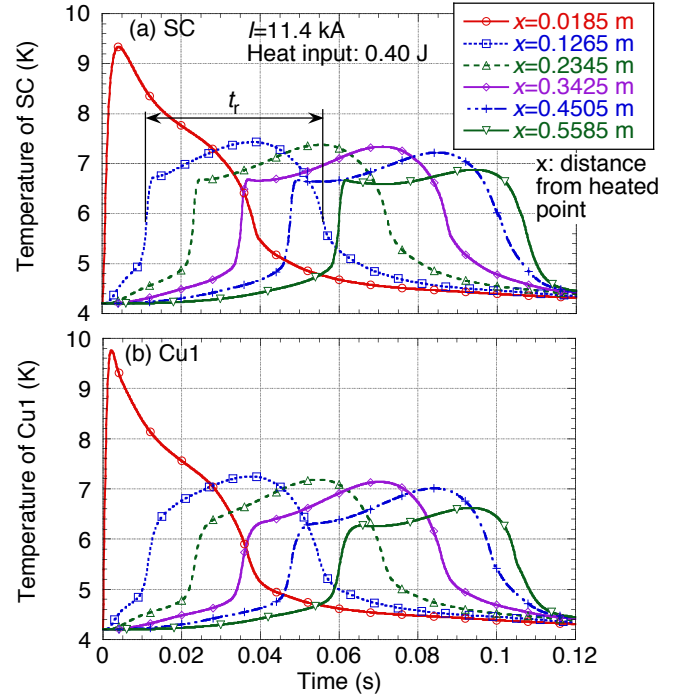
Fig. 11. Calculated temperatures of one-side propagation of a normal zone at 11.4 kA with $K_{12}/K_{23}/K_{34}/K_{45}$ =100/20/100/50 W/m/K, HF=0.95, the initial helium temperature of 4.2 K and the saturated temperature of 4.4 K. The temperature at x=0.0185 m is affected by the heater.

IV. CONCLUSION

Propagation of a short normal zone was observed in an LHD helical coil cooled with subcooled helium. Such short propagating normal zones were also observed in the model coil. Propagating normal zones in subcooled helium are shorter than in saturated helium in spite of the higher operating current. In subcooled helium, the recovery starts within 0.02-0.03 s after the normal transition. It is shorter than the time constant of current diffusion into the aluminum stabilizer. According to the simulation of the propagation of a normal zone, it is considered that such a short normal zone propagates without full transition to film boiling. The temperature rise in the oxidized surface of the conductor allows normal transition under good heat transfer.

REFERENCES

[1] A. Komori, H. Yamada, S. Imagawa, O. Kaneko, K. Kawahata, K. Mutoh, et al., "Goal and achievements of Large Helical Device project," *Fusion Science and Technology*, vol. 58, pp. 1-11, July 2010.

[2] S. Imagawa, T. Mito, K. Takahata, S. Yamada, N. Yanagi, H. Chikaraishi, R. Maekawa, H. Tamura, A. Iwamoto, S. Hamaguchi, T. Obana, T. Okamura, Y. Shirai, T. Ise, T. Hamajima, LHD Experiment Group, "Overview of LHD Superconducting Magnet System and Its 10-Year Operation," *Fusion Science and Technology*, vol. 58, pp. 560-570, July 2010.

[3] N. Yanagi, T. Mito, S. Imagawa, K. Takahata, T. Satow, J. Yamamoto, O. Motojima and The LHD Group, "Development and quality control of the superconductors for the helical coils of LHD," *Fusion Eng. Des*. vol. 41, pp. 241-246, Sep. 1998.

[4] N. Yanagi, S. Imagawa, Y. Hishinuma, K. Seo, K. Takahata, S. Hamaguchi, A. Iwamoto, H. Chikaraishi, H. Tamura, S. Moriuchi, S. Yamada, A. Nishimura, T. Mito, O. Motojima, "Asymmetrical normal-zone propagation observed in the aluminum-stabilized superconductor for the LHD helical coils," *IEEE Trans. Appl. Supercond*. vol. 14, pp. 1507-1510, June 2004.

[5] N. Kawawada, S. Noguchi, H. Igarashi, A. Ishiyama, N. Yanagi, and S. Imagawa, "Transient stability analysis taking into account Hall effect for large aluminum stabilized superconductor," *IEEE Trans. Appl. Supercond*. vol. 16, pp. 1717-1720, June 2006.

[6] Y. Shirai, R. Ikuta, T. Goto, M. Ohya, M. Shiotsu, S. Imagawa, "Transient stability analysis of large scale aluminum stabilized superconductor cooled by He II," *IEEE Trans. Appl. Supercond*. vol. 18, pp. 1275 - 1279, June 2008.

[7] S. Imagawa, "Dynamic analysis of the propagation velocity of the LHD helical coil", Proc. 24th International Cryogenic Engineering Conference and International Cryogenic Material Conference 2012 (Fukuoka, Japan, May 14-18, 2012) pp. 591-594, 2013.

[8] S. Imagawa, S. Hamaguchi, N. Yanagi, H. Sekiguchi, S. Moriuchi, T. Mito, A. Komori, O. Motojima, "Upgrading program for improving the cryogenic stability of LHD helical coils by lowering the operating temperature," *Fusion Eng. Des*. vol. 81, pp. 2583-2588, Nov. 2006.

[9] S. Imagawa, N. Yanagi, Y. Hishinuma, T. Mito, K. Takahata, H. Chikaraishi, H. Tamura, A. Iwamoto, S. Hamaguchi, K. Seo, S. Yamada, A. Nishimura, and O. Motojima, "Results of stability test in subcooled helium for the R&D coil of the LHD helical coil," *IEEE Trans. Appl. Supercond*. vol. 14, pp.1511-1514, June 2004.

[10] S. Imagawa, N. Yanagi, and T. Mito, "Reconsideration of evaluation of balance voltages during a normal zone propagation in the LHD helical coils," *IEEE Trans. Appl. Supercond*. vol. 23, June 2013, Art. No. 4700904.

[11] S. Imagawa, N. Yanagi, and T. Mito, "Detection system of a propagating normal-zone with pick-up coils in the LHD helical coils," *IEEE Trans. Appl. Supercond*. vol. 21, pp. 2316-2319, June 2011.

[12] A. Devred, "Investigation of current redistribution in superstablized superconducting winding when switching to the normal resistive state," *J. Appl. Phys*. vol. 65, no. 10, pp. 3963-3967, May 1989.

[13] C.A. Luongo et al. "Current Diffusion Effects on the Performance of Large Monolithic Conductors," *IEEE Trans. Magn*. vol. 25, pp. 1576-1581, Mar. 1989.

[14] A. Lee, R. H. Wands, and R. W. Fast, "Study of current redistribution in aluminum stabilized superconductor," *Cryogenics*, vol. 32, no. 10, pp. 863-866, 1992.

[15] L. Dresner, "Superconductor stability '90: a review," *Cryogenics*, vol. 31, Issue 7, pp. 489-498, July 1991.

[16] Nick, W. and Schmidt, C., "Thermal magnetoresistance of copper matrix in compound superconductor, a new measuring method," *IEEE Trans. Magn*. vol. 17, pp. 217-219, Jan. 1981.

[17] Iwamoto, A., Maekawa, R. and Mito, T., "Steady state heat transfer of an oxidized copper surface in subcooled liquid helium," *Fusion Eng. Des*. vol. 81, pp. 2611-2615, Nov. 2006.

[18] Bishoff, J., Vassilev, P.G. and Goncharov, I.N., "Low temperature heat capacity of Nb-79.6 wt% Zr, Nb-38 wt% Ti and multifilamentary cables of NT-50," *Cryogenics*, vol. 22, pp. 131-134, Mar. 1982.